ACI STRUCTURAL JOURNAL TECHNICAL PAPER

Title no. 103-S29

Lap Splices Anchored by Headed Bars

by M. Keith Thompson, Antonio Ledesma, James O. Jirsa, and John E. Breen

The anchorage behavior of headed reinforcement in lap splices was studied experimentally. Observations of cracking behavior, strain measurements of reinforcement, and strength are reported. The behavior of unconfined laps is compared to confined laps. The behavior of nonheaded and headed bar laps is compared. Bar stresses are compared with a proposed model for bearing capacity at the head.

Test results suggest that noncontact lap splices should be modeled using a truss mechanism with diagonal compression struts between opposing bars. Under such a model, the capacity of the lap is determined by an anchorage length that is defined by the intersection points of the diagonal struts. Using this model, the anchorage behavior of headed bars is similar to previously reported results from CCT node tests wherein anchorage consisted of bond and head bearing components. Overall results demonstrate that headed reinforcement can significantly reduce the required lap length of spliced reinforcement.

Keywords: anchorage; lap splice; reinforcement; strut.

INTRODUCTION

The Texas Department of Transportation (TxDOT) funded a program to study the feasibility of headed reinforcement in bridge structures. One potential application of interest was to reduce the length of cast-in-place joints between precast elements. For precast elements in which mild reinforcement must be made continuous, cast-in-place joints must be used between the precast units in order to accommodate lapping of longitudinal reinforcement. The length of the cast-in-place joint is dictated by the required lap splice length. Headed ends could be used on the longitudinal reinforcement to reduce the required lap length and shorten the cast-in-place joint (Fig. 1).

In a companion study, the behavior of headed reinforcement in compression-compression-tension (CCT) nodes[1,2] was examined. CCT nodes represent a localized region in which two intersecting compression fields in a concrete region are equilibrated by a layer of reinforcement in tension. Additional background on the various types of nodes and the process of strut-and-tie modeling can be found in Appendix A of ACI 318-02.[3] Some results from the CCT node study are relevant for the material presented in this paper:

- Headed bars anchored at CCT nodes have two components of anchorage: bond and head bearing. These components develop in separate stages. Anchorage is first carried by bond. Bond eventually reaches a peak capacity and begins to decline. As bond capacity declines, bar stress is transferred to the head, causing a rapid rise in head bearing. Failure occurs when head bearing reaches an ultimate capacity. The final anchorage capacity is a combination of peak head bearing and reduced bond;
- Failure bond stress is inversely proportional to the size of the head. The greater the relative head area, the less the bond stress at failure. (Note: relative head area is a nondimensional ratio used to characterize the size of the head. Relative head area is defined as the ratio of net head area A_{nh} to the bar area A_b.); and
- A model was proposed for calculating the force provided by head bearing. The proposed model is based on existing ACI code equations[3] for bearing strength and side blowout capacity.

$$\text{Bearing pressure, } \frac{N}{A_{nh}} = 0.9 f_c' \left(\frac{2c}{\sqrt{A_{nh}}}\right)\Psi \tag{1}$$

$$\text{where } \Psi = 0.6 + 0.4\left(\frac{c_2}{c}\right) \le 2.0 \tag{2}$$

Equation (1) and (2) are for calculating mean capacity. A reduction factor of 0.7 is applied to Eq. (1) to adjust the model such that 95% of test results are equal to or greater than the computed capacity.

The behavior of headed bars in lap splices is compared to the behavior and trends observed in the CCT node study. Additionally, the proposed model for head capacity is compared with data from the lap splice study.

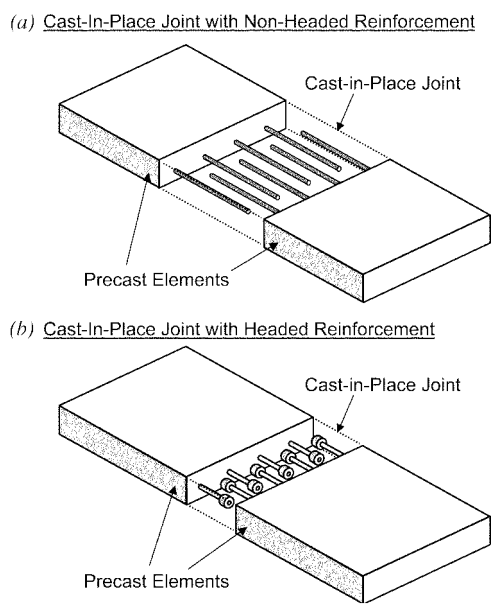

Fig. 1—Reduction of cast-in-place joint by using lap splice with headed reinforcement.

ACI Structural Journal, V. 103, No. 2, March-April 2006.
MS No. 04-318 received October 1, 2004, and reviewed under Institute publication policies. Copyright © 2006, American Concrete Institute. All rights reserved, including the making of copies unless permission is obtained from the copyright proprietors. Pertinent discussion including author's closure, if any, will be published in the January-February 2007 *ACI Structural Journal* if the discussion is received by September 1, 2006.

ACI member **M. Keith Thompson** *is an assistant professor at the University of Wisconsin-Platteville, Platteville, Wis. He received his BS from North Carolina State University, Raleigh, N.C., and his MS and PhD from the University of Texas at Austin, Austin, Tex. His research interests include anchorage of reinforcement and strut-and-tie modeling.*

ACI member **Antonio Ledesma** *is a structural engineer for Parsons Brinkerhoff Quade and Douglas, Tampa, Fla. He received his BS from North Carolina State University and his MS from the University of Texas at Austin.*

James O. Jirsa, *FACI, holds the Janet S. Cockrell Centennial Chair in Engineering at the University of Texas at Austin. He is a Past President of ACI, a member of the ACI Board of Direction, and a Past Chair of the Technical Activities Committee. He is a member of ACI Committees 318, Structural Concrete Building Code; 408, Bond and Development of Reinforcement; and is a member and Chair of Subcommittee 318-F, New Materials, Products, and Ideas (Structural Concrete Building Code).*

ACI Honorary Member **John E. Breen** *holds the Nasser I. Al-Rashid Chair in Civil Engineering at the University of Texas at Austin. He is a member and Past Chair of ACI Committee 318, Structural Concrete Building Code; is a member of ACI Committees 318-B, Reinforcement and Development; 318-E, Shear and Torsion; and 355, Anchorage to Concrete; and is a Past Chair of the Technical Activities Committee.*

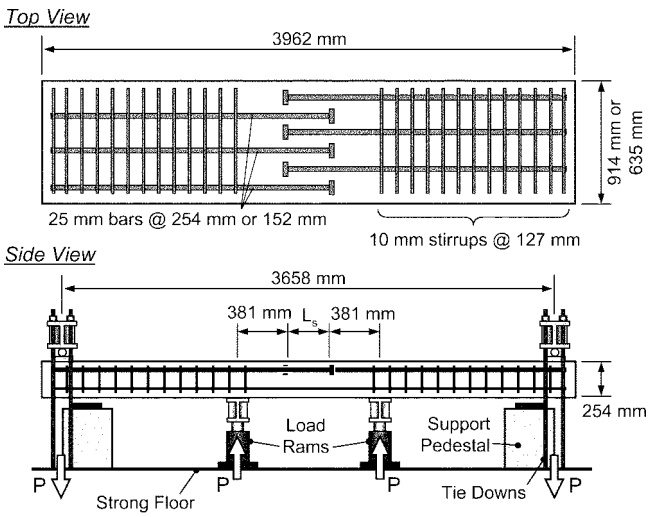

Fig. 2—Typical lap splice specimen.

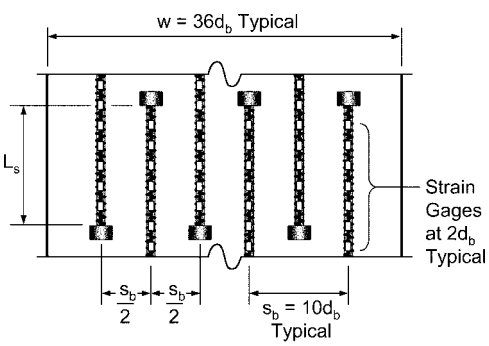

Fig. 3–Detail of lap zone.

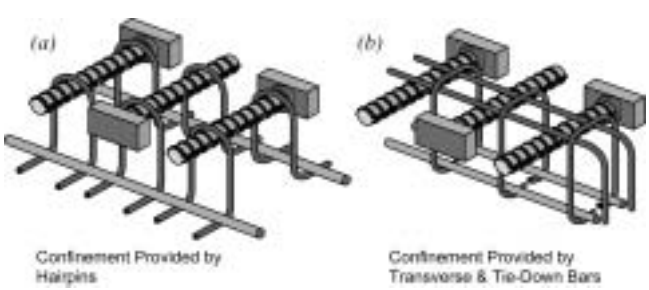

Fig. 4—Lap splice confinement details.

RESEARCH SIGNIFICANCE

Twenty-seven lap splice specimens were tested. These tests provide experimental data on the mechanics of lap splices and anchorage of headed reinforcement. The results of this study augment previous results gathered from a study of headed reinforcement in CCT nodes. Combined with the results of the CCT node study, much needed information on the behavior and capacity of headed reinforcement has been generated.

TEST PROGRAM

A typical lap splice specimen is shown in Fig. 2. Three 25 mm-diameter reinforcing bars were lapped at the midpoint of the specimen. All lapped bars were located in the same plane with an effective depth of 191 mm. The width of the specimen depended upon the bar spacing (914 mm for a bar spacing of 254 mm and 635 mm for a bar spacing of 152 mm). Additionally, four 16 mm diameter bars, placed at a depth close to the neutral axis, provided post-failure integrity to the specimen for handling. Most specimens were unconfined within the lap zone, without stirrups or other supplementary reinforcement used to enhance the performance of the splice. Depending upon the specific structural application, the details of a lap splice may vary tremendously. The configuration used in these test specimens was chosen primarily for its simplicity. Specimen variables are listed below:

- *Splice length* L_s—The lap splice length varied from $3d_b$ to $14d_b$. This range of splice lengths is quite small, but insured that the lap splices would fail before the longitudinal tension steel could yield;
- *Head size and shape*—Three head sizes were tested: nonheaded (A_{nh}/A_b = 0.0), small heads (A_{nh}/A_b = 1.1 to 1.3), and larger heads (A_{nh}/A_b = 4.0 to 4.7). Additionally, circular heads were compared to rectangular heads of approximately the same area;
- *Bar spacing* s_b—Most specimens used a spacing of $10d_b$ between longitudinal bars. A few specimens were fabricated with a spacing of $6d_b$. Specimen width was reduced from $36d_b$ to $25d_b$ to accommodate the smaller spacing;
- *Contact or noncontact lapping*—Lapped bars are typically placed in contact with each other to optimize splice performance. However, for the precast application from which interest in the lap splice tests developed, lapped bars should be placed to avoid contact with one another (refer to Fig. 3). Errors in bar placement during precasting could result in the conflicts between opposing bars when elements are erected. The use of noncontact splices provides the most tolerance for specimen fabrication and enhances constructibility. Thus, most specimens were tested with noncontact splices. Two specimens were tested with contact splices for comparison; and
- *Confinement details*—The effect of confinement was examined in a limited number of specimens. Two confinement details were tested: one using hairpins placed at the ends of the lap zone and another with transverse bars across the lap zone and hoops to tie the concrete cover over the lap zone to the compression zone of the beam. (This second detail is referred to as the transverse tie down detail.) Both details are shown in Fig. 4. The amount of confinement was typically characterized by the area of tie down reinforcement A_{tr} per lapped bar area A_b.

Details of all lap splice specimens are listed in Table 1. Concrete strength was not intended as a variable and was

kept between 22 to 29 MPa for most specimens. Four prototype specimens were tested early in the research that had different details than the typical specimens. These tests were excluded from the general data analysis. Additionally, bond was prevented in one specimen by the use of sheathing placed over the straight bar length within the lap zone.

Instrumentation of the specimens consisted of load-beam deflection measurements and strain measurements along the bars in the lap zone (as shown in Fig. 3). The test setup is shown in Fig. 2. Specimens were loaded from below by four hydraulic rams and tied down at the ends to a reaction floor. This load configuration provided a convenient view of crack patterns. Load was controlled using a manually operated hand pump. Load was increased in 2 kN increments and reduced to 1 kN increments near failure. The total time of testing was approximately 1 hour with several 5-minute pauses for marking cracks and taking photos.

TEST RESULTS

Behavior of unconfined lap splices

Observed Crack Behavior—First cracking in the lap splice specimen usually consisted of transverse flexural cracks outside of the lap zone. Near failure, one or more longitudinal cracks would form over the lapped bars, indicating bond splitting and loss of bond stress. The location of these cracks tended to occur away from the head, near the exit point of the bars from the lap zone. Prior to failure, diagonal cracks propagated from the heads of the bars. Failure occurred with a rapid loss of capacity and extensive propagation of surface cracks over the lap zone (Fig. 5(a)). The direct cause of failure could not be ascertained, but was probably a result of splitting stress at the heads leading to rupture of the cover concrete. Additional deformation was imposed on the specimen after failure until the surface cover spalled completely free of the lap zone and internal cracking could be viewed (Fig. 5(b)).

Several common characteristics of internal cracking were shared among the tests (Fig. 6). On one end of the lap, cracks

Table 1—Summary of lap splice tests

	Head dimensions, mm*	d_b, mm	s_b/d_b	L_s/d_b	L_a†$/d_b$	A_{nh}/A_b	c/d_b	c_2‡$/d_b$	f_c', MPa	A_{tr}§$/A_b$	f_s at $2d_b$, MPa	f_s at L_a, MPa	M_{max}, kN · m
Prototype tests	d_h = 25‖	16	16	12	7	1.39	4.0	4.0	39	0.00	—	—	93.3#
	d_h = 25‖	16	16	12	7	1.39	4.0	4.0	39	0.00	—	—	95.1#
	d_h = 25‖	16	10	12	9	1.39	2.5	4.0	39	0.00	—	—	103.0
	51 x 51‖	16	10	11	8	11.90	2.5	4.0	39	0.00	—	—	122.1#
Unconfined tests	No head	25	10	5	3	0.00	2.5	2.5	22	0.00	6	23	35.2
	No head	25	10	8	6	0.00	2.5	2.5	28	0.00	120	154	53.4
	No head	25	10	12	10	0.00	2.5	2.5	29	0.00	77	262	79.1
	d_h = 38	25	6	3	1.5	1.18	1.5	2.5	26	0.00	62	62	39.2
	d_h = 38	25	10	5	3	1.18	2.5	2.5	26	0.00	58	92	53.9
	d_h = 38‖	25	10	5	3	1.18	2.5	2.5	26	0.00	102	121	55.7
	d_h = 38	25	10	8	6	1.18	2.5	2.5	28	0.00	97	182	65.2
	38 x 76	25	6	3	1.5	4.70	1.5	2.5	22	0.00	128	128	46.9
	38 x 76	25	6	5	3	4.70	2.5	2.5	26	0.00	166	186	64.1
	38 x 76	25	10	5	3	4.70	2.5	2.5	22	0.00	169	166	65.6
	38 x 76‖	25	10	5	3	4.70	2.5	2.5	22	0.00	170	169	74.0
	38 x 76	25	10	8	6	4.70	2.5	2.5	28	0.00	272	300	74.5
	d_h = 57	25	10	8	6	4.04	2.5	2.5	28	0.00	279	306	76.0
	38 x 76	25	10	12	10	4.70	2.5	2.5	29	0.00	292	457	111.4
	d_h = 57	25	10	12	10	4.04	2.5	2.5	26	0.00	287	352	86.4
	d_h = 57	25	10	14	12	4.04	2.5	2.5	24	0.00	270	448	117.4
	d_h = 57**	25	10	14	12	4.04	2.5	5.0	24	0.00	375	375	99.8
Confined tests	No head	25	10	8	6	0.00	2.5	2.5	29	0.25	51	152	59.7
	38 x 76	25	10	8	6	4.70	2.5	2.5	29	0.25	343	378	97.0
	d_h = 57	25	10	8	6	4.04	2.5	2.5	24	0.56	391	373	95.5
	d_h = 57	25	10	8	6	4.04	2.5	2.5	24	1.01	361	391	102.2
	d_h = 57	25	10	12	10	4.04	2.5	2.5	26	0.56	275	371	92.4
	d_h = 57	25	10	12	10	4.04	2.5	2.5	26	0.32††	414	390	100.1

*Diameter d_h is given for circular heads. For rectangular heads, dimensions are given in the order: horizontal × vertical.

†Anchorage length L_a has been estimated using strain data from lap zone. Values provided in table are approximate.

‡Secondary cover dimension c_2 has been estimated as 1/4 bar spacing except for debonded test (refer to footnote **).

§Parameter to characterize confined specimens: area of tie-down reinforcement A_{tr}/area of lapped bars A_b.

‖Contact lap splice. Anchorage length L_a estimated to match companion noncontact splice.

#Lapped bars yielded.

**Debonding sheath placed over bar deformations in lap zone. Secondary cover c_2 estimated as 1/2 bar spacing.

††Transverse tie down confinement detail used. Tie down reinforcement ratio is provided for comparison to tests confined by hairpin reinforcement.

always tended to propagate from the heads to opposing bars at an angle of 55 degrees measured from the bar axis. On the other end of the lap, well-defined wedges formed at the heads of the opposing bars (Fig. 6 and 7). This pattern suggests a mechanism of stress transfer under which the actual length available for anchorage is the lap splice length less the distance necessary for compression struts to propagate from the end of the bar to the shafts of opposing bars (Fig. 8). This result prompted the use of a new term, the anchorage length L_a, which better characterized the behavior and capacity of the lapped bars than the splice length L_s. It should also be noted, that the compliment of this typical 55-degree angle is 35 degrees, the angle commonly found as the slope for breakout cones of headed anchors and used in Appendix D of ACI 318-02[3] (refer to Fig. RD.4.2.2(a) of that code).

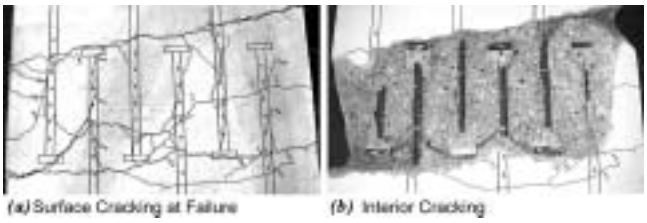

Fig. 5—Typical cracking patterns.

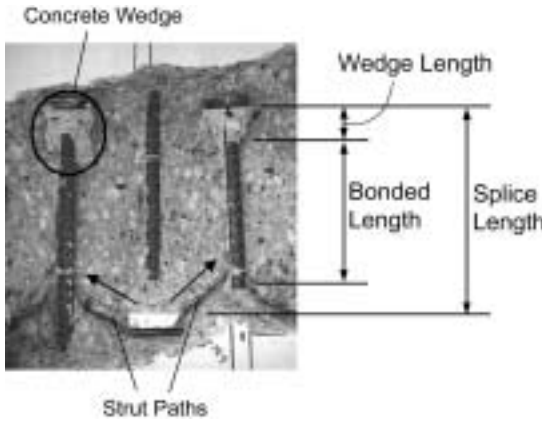

Fig. 6—Close-up of internal cracking.

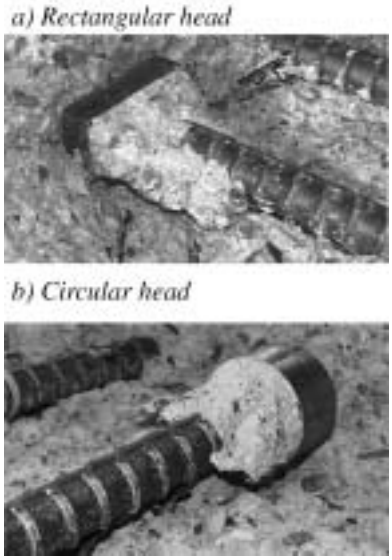

Fig. 7—Concrete wedges.

Bar stresses

The development of bar stress for nonheaded and headed laps is shown in Fig. 9. The data comes from two tests that both had a $12d_b$ splice length L_s, $10d_b$ bar spacing s_b, and concrete strength f_c' equal to 29 MPa. The headed bars had 38 x 76 mm heads, all of which were oriented with the long dimension parallel to the plane of the splice. The stress profiles were recorded at the maximum load carried by each specimen and are averaged from the three bars on either side of the lap splice. The specimen with headed bars reached a maximum bar stress of about 450 MPa, approximately 80% greater than the bar stress attained by the nonheaded bars (around 250 MPa). The heads contributed about 275 MPa of bar stress, while bond contributed 175 MPa. The bond component for the headed bars was less than the bond achieved by the nonheaded bars. This behavior concurs with previous results from tests of CCT nodes anchored by headed reinforcement.[1,2] Using the average stresses from all six bars in the specimen, bond and head bearing components are plotted in Fig. 10. Once again, the plot shows similar trends as data from headed bars anchored in CCT nodes. Anchorage was at first carried by bond, which reached a peak capacity and began to decline. Simultaneously, bar stress was transferred to the head, causing a sharp rise in the head bearing component. Peak capacity was a combination of head bearing plus reduced bond.

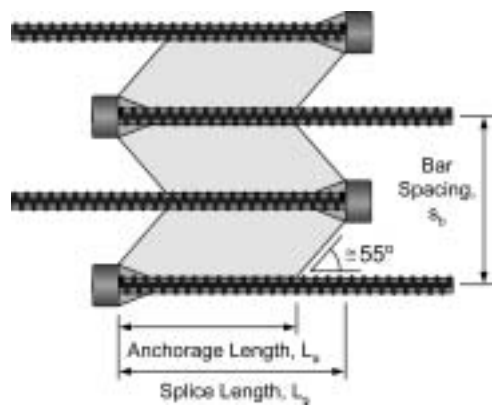

Fig. 8—Mechanism of force transfer between opposing lapped bars.

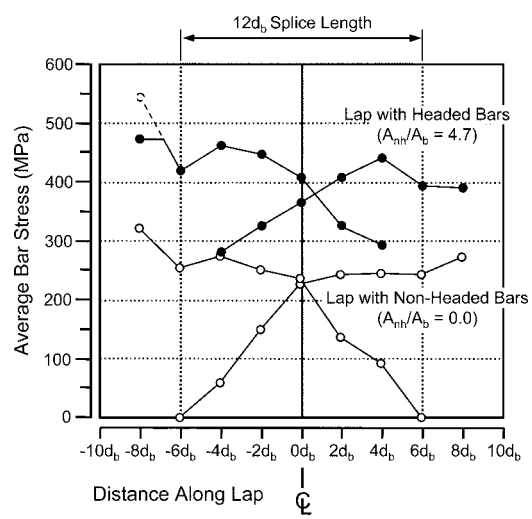

Fig. 9—Bar stress profiles for lap splices with headed and nonheaded bars.

The bar stress data shown in Fig. 9 were used to calculate bond stress profiles, which are plotted in Fig. 11. The bond stress profiles reaffirm observations from the crack behavior. For both the headed and nonheaded bars, bond stress passed through zero at a point corresponding with the end of the anchorage length observed from the internal crack pattern (about $10d_b$ from the face of the head). In the headed bar profile, the trend of the leftmost data points indicates that bond tapered to zero at a distance approximately equal to the wedge length from the head.

Trends in behavior—Maximum bar stress is plotted against lap splice length in Fig. 12. Capacity generally increased with increasing splice length and increasing head size. A secondary scale shows the approximate anchorage length, based on an assumption that the longitudinal distance necessary for diagonal compression struts to propagate between opposing bars was about $2d_b$ for all specimens. Using zero anchorage length as the origin, a trend line was drawn that matched the nonheaded bar data. A parallel trend line fit the headed bar data very well. The offset between the nonheaded trend line and the trend line for the bars with larger heads was about 150 MPa, the stress that was contributed by the addition of the larger head size.

Additional trends were observed from various groups of companion specimens (albeit with limited scope):

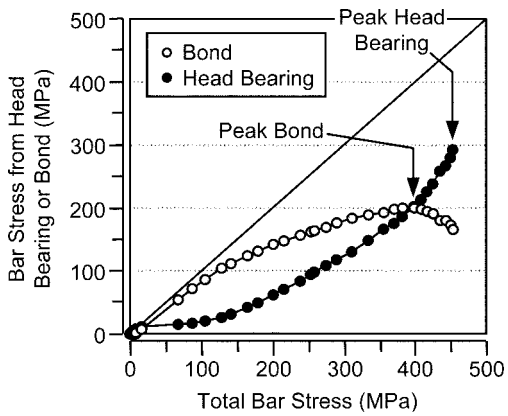

Fig. 10—Bond and head bearing components of anchorage.

- Results from one pair of companion tests with similar head areas showed that head shape had no significant effect on capacity;
- Results from two pairs of companion tests showed that contact lap splices had slightly greater capacity than noncontact splices. The increase in bar stress was significant for small heads, but negligible for larger heads. Larger heads tend to impose an unavoidable separation between the shafts of lapped bars due to the space required for the head dimensions. Thus, for larger head sizes, there was less difference between contact and noncontact lap configurations. Additionally, tests with contact lap splices demonstrated less cracking in the lap zone than tests with noncontact lap splices; and
- Results from one pair of companion tests showed that capacity decreased slightly as bar spacing was reduced.

Behavior of confined lap splices

Two confinement details were tested: hairpins and the transverse tie-down detail (refer to Fig. 4). Hairpins were selected because this detail was considered to best address the mode of failure for the lap splices, rupture of the cover concrete due to splitting stress produced by the head, and because the detail was simple. The transverse tie-down detail was later selected as an alternative approach that provided: 1) transverse bars to balance the compression struts of the truss model for the outside bars of the lap zone; and 2) tie-down bars to connect the lap zone to the compression zone of the beam, thus preventing rupture of the concrete cover. The hairpins were tested with various bar sizes (4.7, 10, and 13 mm diameters) and two different splice lengths ($8d_b$ and $12d_b$). The transverse tie-down detail was fabricated from 10 mm-diameter deformed bars and used only once with a $12d_b$ splice length.

Cracking of the hairpin-confined specimens closely resembled cracking in companion unconfined specimens. Failure occurred much the same way as unconfined tests with rapid loss of strength and propagation of multiple surface cracks over the lap zone. Failure of the specimen with the transverse tie-down detail was more gradual with some improvement in deformation ability. Additionally, spalling of the cover concrete was prevented even after large

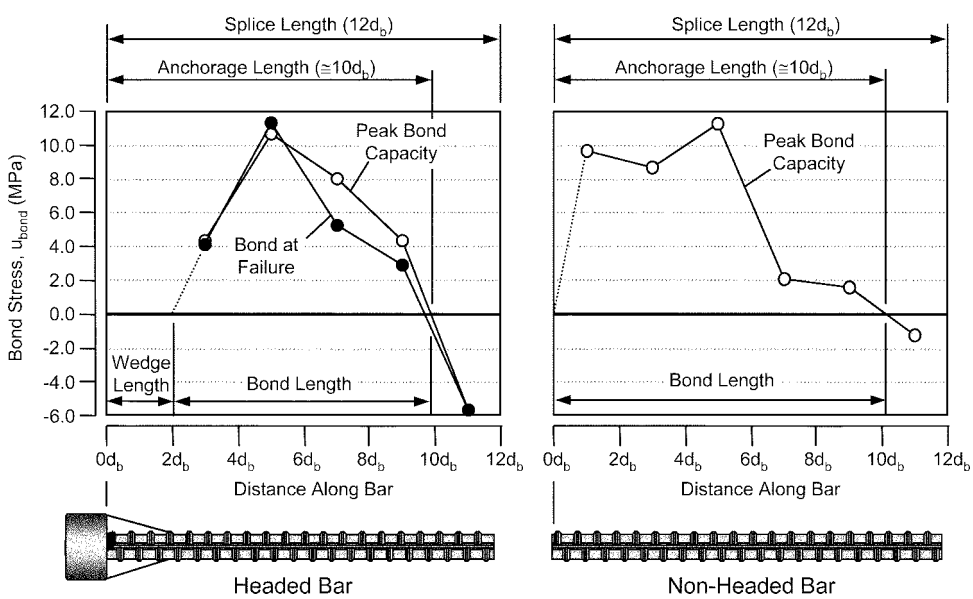

Fig. 11—Bond stress profiles for lap splices with headed and nonheaded bars.

deformations were imposed on the specimen. Load-deflection plots for unconfined, hairpin-confined, and the transverse tie-down specimens (with larger heads and $12d_b$ splice length) reveal the changes in capacity and ductility provided by each detail (Fig. 13).

Bond profiles

Perhaps the most revealing data on the effects of confinement were provided when bond stress profiles were calculated (Fig. 14). The bond stress profiles for the hairpin-confined tests were very similar to the bond stress profiles for companion unconfined, headed bar tests (refer to Fig. 11). The scale diagram below the plot shows the positions of the two hairpins relative to the bond length of the bar. The figure shows that the hairpins were placed outside of the bond length, eliminating much of their potential benefit. One hairpin was placed within one bar diameter of the head (inside the wedge length) and the second was placed one bar diameter from the boundary of the lap zone (outside of the anchorage length as it turned out). Internal crack patterns revealed this as well (Fig. 15). This poor placement of the hairpins occurred because a complete understanding of the mechanics of stress transfer in the lap zone was lacking at the time the hairpin tests were designed. The hairpin placed next to the head did not significantly improve the head bearing contribution of anchorage and the other hairpin was not placed along any critical portion of the bar shaft. The hairpin detail may have been more effective if placed within the bond length of the lapped bars. These results serve as a warning that confining reinforcement is not effective if poorly placed and demonstrate the value of tests to understand the manner in which supplementary reinforcement improves anchorage.

The bond stress profile for the test with the transverse tie-down detail showed significant differences from the unconfined and hairpin-confined tests. The bond stress at failure significantly deteriorated from the value at peak bond. Furthermore, the anchorage length contracted as well, possibly indicating a change in the truss mechanism through

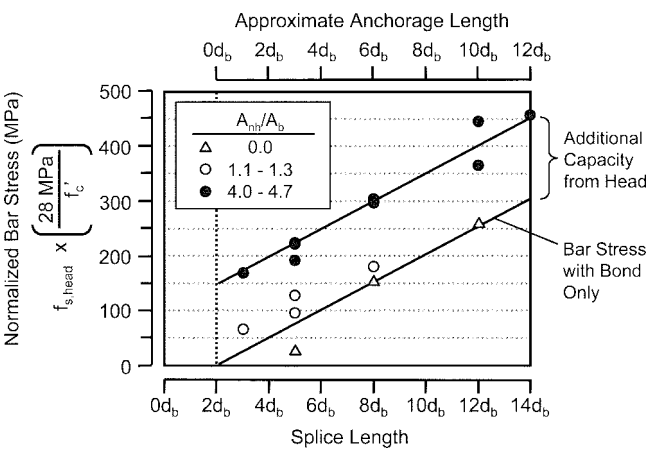

Fig. 12—Cumulative unconfined lap splice data.

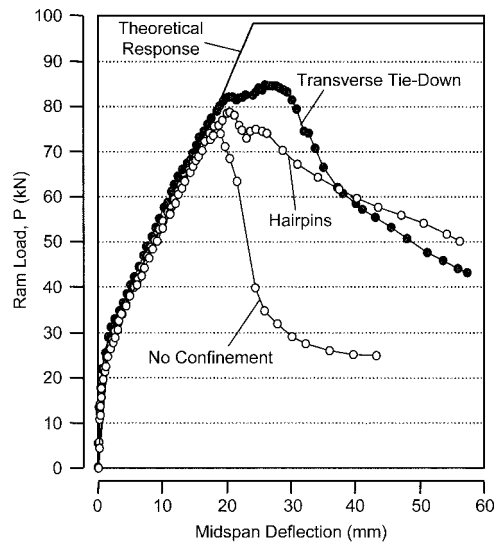

Fig. 13—Load-deflection curves for confined and unconfined specimens.

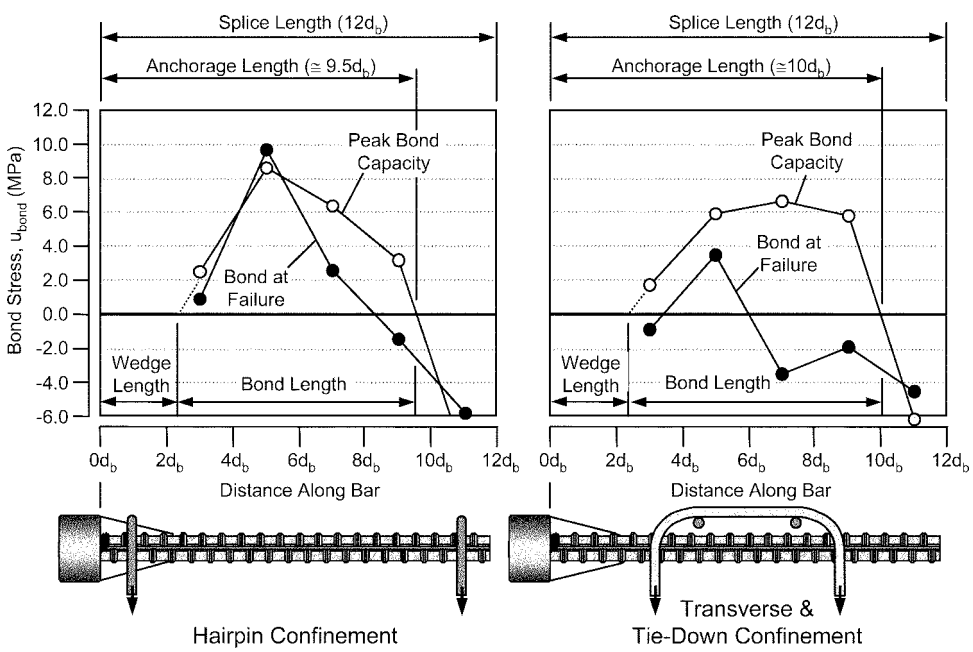

Fig. 14—Bond stress profiles for confined lap splices.

which force was transferred between opposing bars. Bond was essentially exhausted when failure occurred. The capacity provided by the transverse tie-down detail is compared with companion unconfined and hairpin-confined specimens in Fig. 16. Whereas both the unconfined and hairpin-confined specimens reached peak capacities with small but significant contributions from bond, the transverse tie-down detail achieved a larger overall capacity comprised entirely from head bearing. Strain gauges placed on the transverse and tie-down bars showed that the transverse bars were much more active than the tie-down bars as bar stress developed at the heads (Fig. 17). The transverse bars were engaged more quickly than the tie-down bars, most likely due to their placement within the plane of the truss mechanism of the lap splice.

One last feature of the transverse tie-down detail deserves mention. Both the transverse tie-down detail and the hairpin bars used in the specimens featured in Fig. 17 used exactly the same overall length as the 10 mm-diameter bar. There was no difference in the amount of reinforcement used in each detail. The difference between the two details was the placement of confining reinforcement. Placement of the confining reinforcement was as (or more) important than the amount used.

Comparison of data to proposed model

A proposed model for head bearing was developed as part of a study of CCT nodes anchored by headed reinforcement.[2]

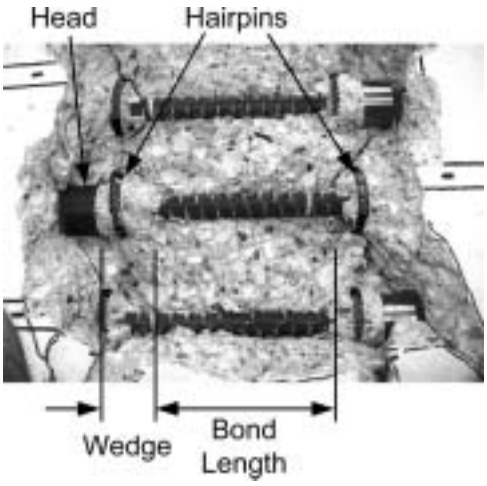

Fig. 15—Internal crack pattern for lap splice with hairpin confinement.

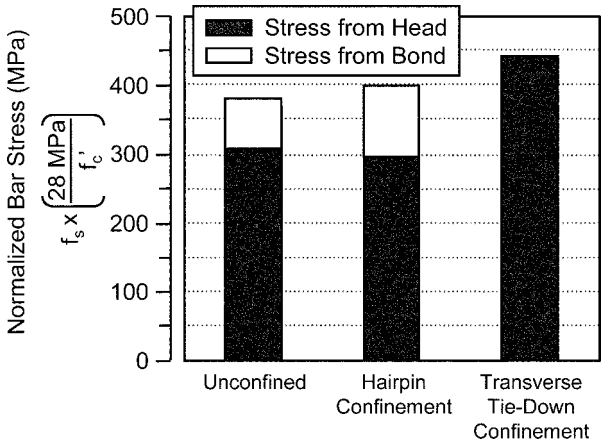

Fig. 16 —Capacities of confined and unconfined lap splices.

Data from the lap splice tests were compared to calculated results from this model, which is presented in Eq. (1) and (2). The proposed model depends on net head area A_{nh}, concrete strength f'_c, minimum cover dimension c, and the minimum cover dimension measured perpendicular to c (c_2). For the lap splice tests, the minimum cover dimension was measured from the center of the bar to the surface of the concrete cover directly over the bars (refer to Fig. 18), while c_2 was taken as half of the center-to-center spacing between opposing bars (or $s_b/4$).

The dimension used for c_2 was selected after analysis showed that this value produced a reasonable match between calculated results and the data for the lap tests. The rational for the use of half the space between opposing bars rather than the full space is that bond in the opposing bars causes splitting cracks that reduce the effectiveness of concrete near the heads. Support of this theory was provided by one test in which a wrap was placed over the shafts of the lapped bars to prevent bond. In this test, splitting cracks were prevented and the value for c_2 was taken as the full space between opposing bars ($c_2 = s_b/2$). For the debonded test, the cover ratio c_2/c was 2.0, making the value of the radial disturbance factor Ψ equal to 1.4. Thus, a 40% increase in bar stress at the head was expected when data from the debonded test was compared with companion tests with full bond, and indeed this was the case. Average bar stress from bonded and

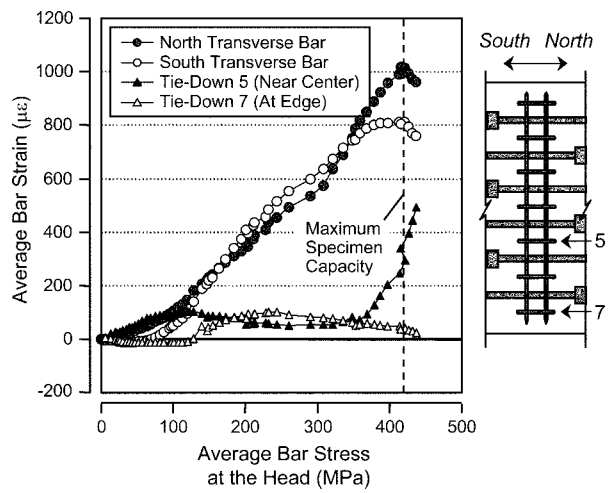

Fig. 17—Bar strains for confining steel of transverse tie-down detail.

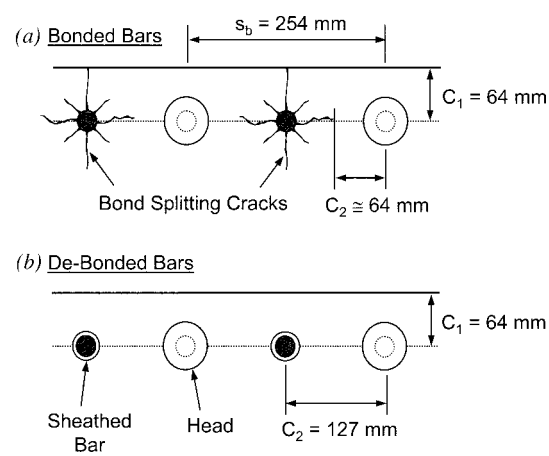

Fig. 18—Cover dimensions for heads in lap splice tests.

debonded specimens is compared in Fig. 19. Normalized bar stress from head bearing was 315 MPa for the bonded specimen and 438 MPa for the debonded specimen, a 39% increase. Note that while the debonded specimen had a higher contribution from head bearing, the bonded specimen had the higher overall capacity because of the presence of bond.

Bar stress at the head was calculated for four unconfined lap tests with small heads and 10 unconfined lap tests with larger heads. Ratios of measured to calculated capacity for these tests are plotted against splice length in Fig. 20. For larger heads at longer splice lengths (six tests from the database), the proposed model performed well with measured to calculated ratios between 0.90 and 1.08. For all other tests, the proposed model provided unsafe calculations of head capacity. The data show a general trend of decreasing capacity with decreasing splice length.

A similar result was reported by Adebar and Zhou[4] who tested unconfined struts and developed a model for strut capacity dependent on many of the same parameters as the proposed model for head capacity. For struts with length/width ratios below 4.0, strut capacity decreases linearly as the length/width ratio of the strut (h/b) decreases:

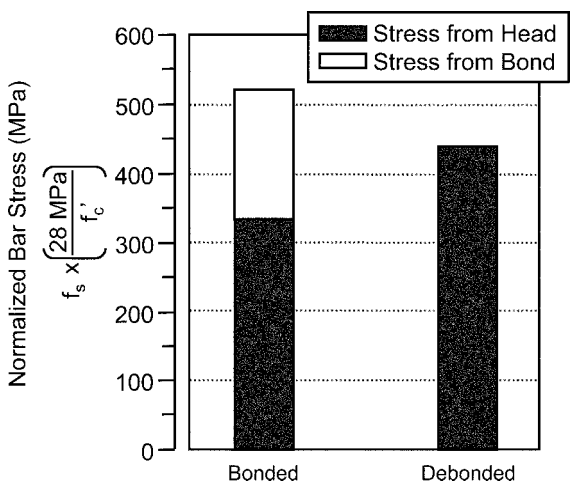

Fig. 19—Capacities of bonded and debonded lap splices.

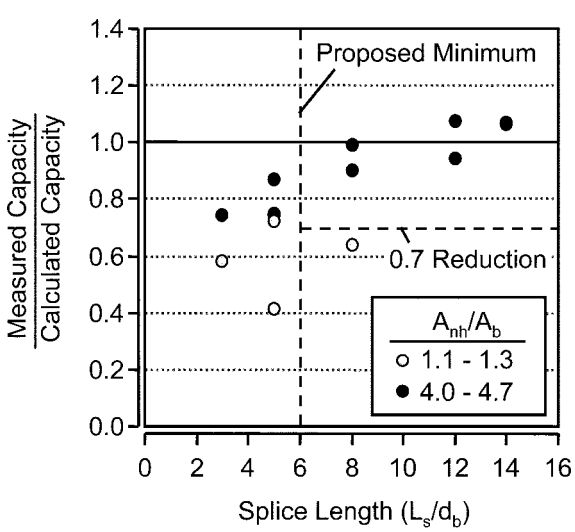

Fig. 20—Performance of proposed model for head capacity with respect to splice length.

$$\text{Bearing pressure, } \frac{N}{A_{nh}} = 0.6 f'_c\,(1 + 2\alpha\beta) \tag{3}$$

$$\text{where} \quad \alpha = 0.33\left(\sqrt{\frac{A_2}{A_{nh}}} - 1\right) \le 1.0 \tag{4}$$

$$\beta = 0.33\left(\frac{h}{b} - 1\right) \le 1.0 \tag{5}$$

The trend recognized by the β term in Adebar and Zhou's model is similar to the trend of the lap splice data. The capacity of the heads decreased as splice length decreased. Two parameters change as the splice length shortens, the anchorage length shortens and the length of the compression struts between opposing heads shortens. One of these parameters probably has an effect on head capacity that is not recognized by the proposed model in its current form. However, provided the anchorage length is greater than a certain limit, the effect is not harmful. A minimum requirement for anchorage length may be sufficient to address applicability of the proposed model. For the CCT node tests from which the model was developed,[2] the minimum anchorage length was about $6d_b$. This limit would be sufficient to exclude the majority of tests from the lap splice study for which the proposed head bearing model was unconservative. When considered in the context of a CCT node, this limit should be thought of as the length necessary to ensure development of a proper node.

Omitting lap tests with anchorage lengths less than $6d_b$, seven tests remained for comparison with the proposed model: one with a small head and six with larger heads. After applying a recommended reduction factor of 0.7 to the proposed model, the average measured/calculated ratio for these seven tests was 1.36 with a standard deviation of 0.21 (15%). The range was 0.91 to 1.54.

CONCLUSIONS

1. Stress was transferred between opposing bars in noncontact lap splices through struts acting at an angle to the direction of the bar. With this truss model, splice capacity was best described using anchorage length and not the length of the lap splice.

2. Anchorage length in noncontact lap splices could be determined by drawing the struts between opposing bars propagate at an angle of 55 degrees with respect to the bar axis.

3. The anchorage behavior of headed reinforcement in lap splices was the same as the anchorage behavior of headed bars in CCT nodes. Anchorage components of bond and head bearing develop in separate stages. Anchorage was first carried by bond that eventually reached a peak capacity and began to decline. As bond capacity declined, bar stress was transferred to the head causing a rapid rise in head bearing. Failure occurred when head bearing reached ultimate capacity. The peak anchorage capacity was a combination of peak head bearing and reduced bond.

4. The head bearing capacity in lap splices could be calculated using a model previously proposed for CCT nodes (Eq. (1) and (2)). For anchorage lengths of $6d_b$ or less, the capacity was over-estimated leading to a recommendation that anchorage length must be greater than $6d_b$.

5. Confinement steel in the form of transverse bars over the top of the lap is more effective than details that only tie the cover down to the compression zone of the beam. The development of a truss mechanism can be enhanced through the use of confinement; however, the placement of supplementary reinforcement is critical for realizing the benefits of confinement.

ACKNOWLEDGMENTS

The support of the Texas Department of Transportation and the guidance of the project supervisor D. Van Landuyt is gratefully acknowledged. The test program was conducted at the Ferguson Structural Engineering Laboratory of the University of Texas at Austin. The help of the laboratory staff and special efforts of graduate students M. Ziehl and A. Ledesma were essential to the conduct of the study.

NOTATION

A_b = bar area, mm^2
A_{gh} = gross head area, mm^2
A_{nh} = net head area, $A_{gh} - A_b$, mm^2
A_{tr} = area of confining reinforcement that ties lapped bars to compression zone, mm^2
b = minimum lateral width of strut measured perpendicular to line of force, mm
c = minimum cover dimension, measured to bar center; cover dimensions should be taken as distance measured to nearest edge, or 1/2 of center-to-center spacing between adjacent bars, mm
c_2 = minimum cover dimension, measured in direction orthogonal to c, mm
d = distance from extreme compression fiber to center of longitudinal reinforcement, mm
d_b = bar diameter, mm
f_c' = concrete compression strength, from cylinder tests, MPa
f_s = bar stress, in general, MPa
$f_{s,bond}$ = bar stress provided by bond, MPa
$f_{s,head}$ = bar stress provided by head bearing, MPa
h = length of strut along the line of force, mm
L_a = anchorage length, measured from point at which tie bar first intersects strut boundary to end of tie bar, mm
L_s = lap splice length, measured between head faces, mm
P = bearing reaction at CCT node, kN
s_b = center-to-center spacing between bars in layer, mm
u_{bond} = average bond stress along bar, MPa
θ_{strut} = strut angle, measured between axis of tie bar and axis of strut
Ψ = radial disturbance factor, $0.6 + 0.4(c/c_2) \leq 2.0$

REFERENCES

1. Thompson, M. K.; Ziehl, M. J.; Jirsa, J. O.; and Breen, J. E., "CCT Nodes Anchored by Headed Bars—Part 1: Behavior of Nodes," *ACI Structural Journal*, V. 102, No. 6, Nov.-Dec. 2005, pp. 808-815.

2. Thompson, M. K.; Jirsa, J. O.; and Breen, J. E., "CCT Nodes Anchored by Headed Bars—Part 2: Capacity of Nodes," *ACI Structural Journal*, V. 103, No. 1, Jan.-Feb. 2006, pp. 65-73.

3. ACI Committee 318, "Building Code Requirements for Structural Concrete (ACI 318-02) and Commentary (318R-02)," American Concrete Institute, Farmington Hills, Mich., Oct. 2002, 443 pp.

4. Adebar, P., and Zhou, Z., "Bearing Strength of Compressive Struts Confined by Plain Concrete," *ACI Structural Journal*, V. 90, No. 5, Sept.-Oct. 1993, pp. 534-541.

5. Thompson, M. K.; Jirsa, J. O.; Breen, J. E.; and Klingner, R. E., "Anchorage Behavior of Headed Reinforcement: Literature Review," *Center for Transportation Research Report* 1855-1, Austin, Tex., May 2002, 112 pp.

6. Thompson, M. K.; Young, M. J.; Jirsa, J. O.; Breen, J. E.; and Klingner, R. E., "Anchorage of Headed Reinforcement in CCT Nodes," *Center for Transportation Research Report* 1855-2, Austin, Tex., May 2002, 160 pp.

7. Thompson, M. K.; Ledesma, A. L.; Jirsa, J. O.; Breen, J. E.; and Klingner, R. E., "Anchorage Behavior of Headed Reinforcement," *Center for Transportation Research Report* 1855-3, Austin, Tex., May 2002, 122 pp.